

RESEARCH ARTICLE

Implicit Floquet analysis of wind turbines using tangent matrices of a non-linear aeroelastic code

P. F. Skjoldan¹ and M. H. Hansen²¹ Loads, Aerodynamic and Control, Siemens Wind Power A/S, DK-2630 Taastrup, Denmark² Wind Energy Division, National Laboratory for Sustainable Energy, Risø DTU, DK-4000 Roskilde, Denmark

ABSTRACT

The aeroelastic code BHawC for calculation of the dynamic response of a wind turbine uses a non-linear finite element formulation. Most wind turbine stability tools for calculation of the aeroelastic modes are, however, based on separate linearized models. This paper presents an approach to modal analysis where the linear structural model is extracted directly from BHawC using the tangent system matrices when the turbine is in a steady state. A purely structural modal analysis of the periodic system for an isotropic rotor operating at a stationary steady state was performed by eigenvalue analysis after describing the rotor degrees of freedom in the inertial frame with the Coleman transformation. For general anisotropic systems, implicit Floquet analysis, which is less computationally intensive than classical Floquet analysis, was used to extract the least damped modes. Both methods were applied to a model of a three-bladed 2.3 MW Siemens wind turbine model. Frequencies matched individually and with a modal identification on time simulations with the non-linear model. The implicit Floquet analysis performed for an anisotropic system in a periodic steady state showed that the response of a single mode contains multiple harmonic components differing in frequency by the rotor speed. Copyright © 2011 John Wiley & Sons, Ltd.

KEYWORDS

modal analysis; Floquet analysis; rotor dynamics

Correspondence

P. F. Skjoldan, Loads, Aerodynamic and Control, Siemens Wind Power A/S, Dybendalsvænget 3, DK-2630 Taastrup, Denmark.

E-mail: peter.skjoldan@siemens.com

Received 26 June 2010; Revised 7 October 2010; Accepted 12 February 2011

1. INTRODUCTION

Today, advanced non-linear finite element codes^{1–3} are routinely used for load calculations on wind turbines. Most wind turbine stability tools for calculation of the aeroelastic modes are, however, based on separate linearized models. Stability analysis can be divided into three steps: first, a calculation of the steady state; then, a linearization of the equations of motion about the steady state and last, a modal analysis to extract modal frequencies, damping and mode shapes. This paper presents an approach to structural modal analysis applicable to any periodic steady state where the linearization is obtained directly from the non-linear wind turbine aeroelastic code BHawC.³

The equations of motion for a wind turbine operating at a constant mean rotor speed contain periodic coefficients, preventing direct eigenvalue analysis of the system. Most recent wind turbine stability tools^{4–7} incorporate the Coleman transformation, also known as the multiblade coordinate transformation, which describes the rotor degrees of freedom in the inertial frame. This transformation eliminates the periodic coefficients if the system is isotropic, i.e. the rotor consists of identical symmetrically mounted blades, and the environment conditions are symmetric. Floquet analysis is, however, applicable to anisotropic systems and any periodic steady state. It requires integration of the equations of motion over a period of rotor rotation, as many times as there are state variables in the system. Because of the computational burden of this approach, it has only been applied to reduce or simplify wind turbine models with a limited number of degrees of freedom.^{8–10} One way to reduce the computation time is to use the Fast Floquet Theory¹¹ where only one third of the integrations are necessary for a three-bladed isotropic rotor. Another way is to use implicit Floquet analysis¹² where the least damped modes can be extracted after a limited number of integrations.

Stol *et al.*¹³ compare the Floquet analysis with the Coleman transformation approach applied to a periodic steady state, where the remaining periodic coefficients are eliminated by averaging and find small differences in modal frequencies and damping, concluding that it is not necessary to use Floquet analysis.

Another approach to modal analysis is system identification,^{14–16} which operates on the response from numerical simulations or measurements, and no knowledge of the system equations is needed to extract the modal properties. The accuracy of the methods is, however, limited and depends on the chosen excitation.

In this paper, tangent matrices for mass, damping and stiffness are extracted from the aeroelastic code BHawC. If the system is isotropic and the steady state is stationary, the Coleman transformation is applied before extracting the modal parameters by eigenvalue analysis. For an anisotropic system, implicit Floquet analysis is used for the modal analysis. When the system is isotropic, the response of a single mode contains a single harmonic component for tower degrees of freedom and up to three components for the blades. The response of a single mode in the anisotropic system on both blades and tower contains multiple harmonic components differing in frequency by the rotor speed.

Section 2 of this paper describes the BHawC model, and Section 3 explains the methods for modal analysis, the Coleman transformation approach, the implicit Floquet analysis and also the partial Floquet analysis, a system identification technique. In Section 4, the methods are applied to a model of a wind turbine. Section 5 discusses the approaches, and Section 6 concludes the paper.

2. STRUCTURAL MODEL

The BHawC wind turbine aeroelastic code³ is based on a structural finite element model sketched in Figure 1, where the main structural parts, tower, nacelle, shaft, hub and blades, are modelled as two-node 12-degrees of freedom Timoshenko beam elements. The code uses a corotational formulation, where each element has its own coordinate system that rotates with the element. The elastic deformation is described in the element frame, whereas the movement of the element coordinate system accounts for rigid body motion. In this way, a geometrically non-linear model is obtained using linear finite elements.

The configuration of the system, defined by nodal positions \mathbf{p} and orientations \mathbf{q} , nodal velocities $\dot{\mathbf{u}}$ (of both positions and orientations) and nodal accelerations $\ddot{\mathbf{u}}$, must satisfy the equilibrium equation given in global coordinates as

$$\mathbf{f}_{\text{iner}}(\mathbf{p}, \mathbf{q}, \dot{\mathbf{u}}, \ddot{\mathbf{u}}) + \mathbf{f}_{\text{damp}}(\mathbf{q}, \dot{\mathbf{u}}) + \mathbf{f}_{\text{int}}(\mathbf{p}, \mathbf{q}) = \mathbf{f}_{\text{ext}} \quad (1)$$

where \mathbf{f}_{iner} , \mathbf{f}_{damp} , \mathbf{f}_{int} and \mathbf{f}_{ext} are the inertial, damping, internal and external force vectors, respectively, and $\dot{(\)} = d/dt$ denotes a time derivative. The inertial forces depend on the acceleration of the masses, the damping forces are given by viscous damping, the internal forces are due to elastic forces and the external forces contain the aerodynamic forces.¹⁷ To find

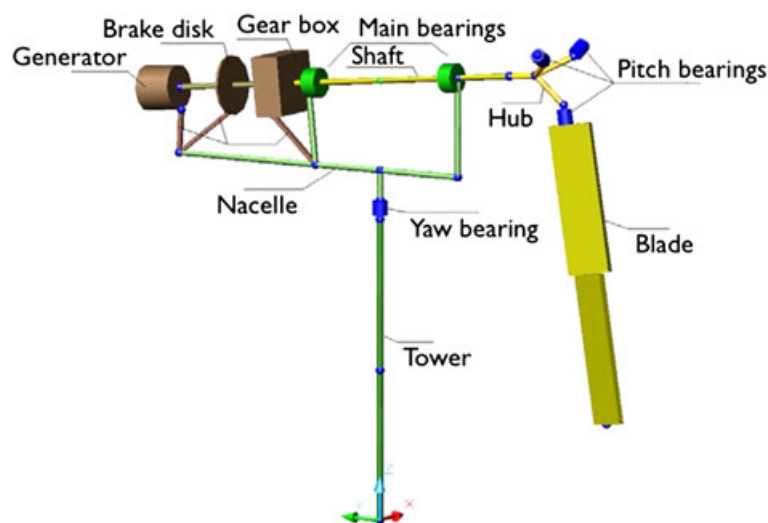


Figure 1. Sketch of the BHawC model substructures.

this equilibrium configuration, increments of the positions and the orientations $\delta\mathbf{u}$, the velocities $\delta\dot{\mathbf{u}}$ and the accelerations $\delta\ddot{\mathbf{u}}$ are obtained using Newton–Raphson iteration with the tangent relation obtained from the variation of Equation (1) as

$$\mathbf{M}(\mathbf{q})\delta\ddot{\mathbf{u}} + \mathbf{C}(\mathbf{q}, \dot{\mathbf{u}})\delta\dot{\mathbf{u}} + \mathbf{K}(\mathbf{p}, \mathbf{q}, \dot{\mathbf{u}}, \ddot{\mathbf{u}})\delta\mathbf{u} = \mathbf{r} \quad (2)$$

where \mathbf{M} , \mathbf{C} and \mathbf{K} are the tangent mass, damping/gyroscopic and stiffness matrices, respectively, and $\mathbf{r} = \mathbf{f}_{\text{ext}} + \mathbf{f}_{\text{iner}} + \mathbf{f}_{\text{damp}} - \mathbf{f}_{\text{int}}$ is the residual. The stiffness matrix is composed of constitutive, geometric and inertial stiffness. The orientation \mathbf{q} of the nodes is described by quaternions, also known as the Euler parameters,¹⁸ a general four-parameter representation equivalent to a triad, which for node number i is updated as

$$\mathbf{q}_i := \text{quat}(\delta\mathbf{u}_{i,\text{rot}}) * \mathbf{q}_i \quad (3)$$

where $\delta\mathbf{u}_{i,\text{rot}}$ contains three rotations that are assumed infinitesimal and thus commute and where this rotation pseudo-vector is transformed by the function termed *quat* into a quaternion, which is used to update the nodal quaternion \mathbf{q}_i employing the special quaternion product denoted by $*$, which maintains the unity of the quaternion. The nodal positions \mathbf{p} , the nodal velocities $\dot{\mathbf{u}}$ and the accelerations $\ddot{\mathbf{u}}$ are updated by regular addition of the positional part of $\delta\mathbf{u}$, $\delta\dot{\mathbf{u}}$ and $\delta\ddot{\mathbf{u}}$, respectively. All components in \mathbf{p} , \mathbf{q} and $\delta\mathbf{u}$ are absolute and described in a global frame.

The present work considers small perturbations in position and orientation \mathbf{y} , velocity $\dot{\mathbf{y}}$ and acceleration $\ddot{\mathbf{y}}$ to a steady state with constant mean rotor speed Ω defined by $(\mathbf{p}_{\text{ss}}, \mathbf{q}_{\text{ss}}, \dot{\mathbf{u}}_{\text{ss}}, \ddot{\mathbf{u}}_{\text{ss}})$, the steady state positions, orientations, velocities and accelerations, respectively, all periodic with the rotor period $T = 2\pi/\Omega$. The linearized equations of motion are obtained from equation (2) at $\mathbf{r} \approx \mathbf{0}$ as

$$\mathbf{M}(\mathbf{q}_{\text{ss}})\ddot{\mathbf{y}} + \mathbf{C}(\mathbf{q}_{\text{ss}}, \dot{\mathbf{u}}_{\text{ss}})\dot{\mathbf{y}} + \mathbf{K}(\mathbf{p}_{\text{ss}}, \mathbf{q}_{\text{ss}}, \dot{\mathbf{u}}_{\text{ss}}, \ddot{\mathbf{u}}_{\text{ss}})\mathbf{y} = \mathbf{0} \quad (4)$$

where the matrices \mathbf{M} , \mathbf{C} and \mathbf{K} are the T -periodic tangent system matrices that are employed in the modal analysis described in the next section.

3. METHODS

In this section, the four methods for modal analysis of structures with rotors are presented.

3.1. Coleman approach

The Coleman transformation requires identical degrees of freedom on each blade, and therefore, the equations of motion (equation (4)) in global coordinates were first transformed into substructure coordinates \mathbf{y}_T . The transformation is

$$\begin{aligned} \mathbf{y} &= \mathbf{T}\mathbf{y}_T \\ \mathbf{T} &= \text{diag}(\mathbf{I}_{N_s}, \mathbf{T}_r, \mathbf{T}_{b1}, \mathbf{T}_{b2}, \mathbf{T}_{b3}) \end{aligned} \quad (5)$$

where \mathbf{T} is a block diagonal time-variant matrix composed of the identity matrix \mathbf{I}_{N_s} sized by the number of degrees of freedom of the tower, the nacelle and the drivetrain, \mathbf{T}_r transforms the degrees of freedom on the shaft and the hub into a hub centre frame and \mathbf{T}_{bj} transforms the degrees of freedom on blade number $j = 1, 2, 3$ into a local frame for blade j . The triads were obtained in the periodic steady state, and thus, \mathbf{T} is T -periodic.

The time-variant transformation into inertial frame coordinates \mathbf{z} is

$$\begin{aligned} \mathbf{y}_T &= \mathbf{B}\mathbf{z} \\ \mathbf{B} &= \text{diag}(\mathbf{I}_{N_s}, \mathbf{B}_r, \mathbf{B}_b) \end{aligned} \quad (6)$$

where \mathbf{B}_r is a simple rotational transformation of the shaft and the hub and \mathbf{B}_b is the Coleman transformation introducing multiblade coordinates for a three-bladed rotor^{11,19} as

$$\mathbf{B}_b = \begin{bmatrix} \mathbf{I}_{N_b} & \mathbf{I}_{N_b} \cos \psi_1 & \mathbf{I}_{N_b} \sin \psi_1 \\ \mathbf{I}_{N_b} & \mathbf{I}_{N_b} \cos \psi_2 & \mathbf{I}_{N_b} \sin \psi_2 \\ \mathbf{I}_{N_b} & \mathbf{I}_{N_b} \cos \psi_3 & \mathbf{I}_{N_b} \sin \psi_3 \end{bmatrix} \quad (7)$$

where $\psi_j = \Omega t + 2\pi(j-1)/3$ is the mean azimuth angle to blade number j and N_b is the number of degrees of freedom on each blade. The inertial frame coordinate vector

$$\mathbf{z} = \{\mathbf{y}_s^T, \mathbf{z}_r^T, \mathbf{a}_0^T, \mathbf{a}_1^T, \mathbf{b}_1^T\}^T \quad (8)$$

contains the untransformed coordinates for tower, nacelle and drivetrain y_s , the coordinates for shaft and hub z_r measured in a non-rotating frame aligned with the hub and the multiblade symmetric coordinates a_0 , cosine coordinates a_1 and sine coordinates b_1 . The details on how multiblade coordinates describe the motion of a wind turbine rotor in the inertial frame are discussed by Hansen.^{20,21}

The Coleman transformed equations were obtained by first inserting equation (5) into equation (4), then converting it to first order form and lastly introducing the inertial frame transformation in equation (6) as $y_{T2} = \mathbf{diag}(\mathbf{B}, \mathbf{B})z_2$ where $y_{T2} = \{y^T \dot{y}^T\}^T$ and $z_2 = \{z^T \dot{z}^T\}^T$ are the state vectors in substructure and inertial frames, respectively, with $\tilde{z} = \dot{z} + \bar{\omega}z$ and the constant matrix $\bar{\omega} = \mathbf{B}^{-1}\mathbf{B}$. The result is

$$\begin{aligned} \dot{z}_2 &= \mathbf{A}_B z_2 \\ \mathbf{A}_B &= \begin{bmatrix} -\bar{\omega} & \mathbf{I} \\ -\mathbf{M}_B^{-1}\mathbf{K}_B & -\mathbf{M}_B^{-1}\mathbf{C}_B - \bar{\omega} \end{bmatrix} \end{aligned} \quad (9)$$

where \mathbf{A}_B is the Coleman transformed system matrix and

$$\begin{aligned} \mathbf{M}_B &= \mathbf{B}^{-1}\mathbf{T}^T\mathbf{M}\mathbf{T}\mathbf{B} \\ \mathbf{C}_B &= \mathbf{B}^{-1}\mathbf{T}^T(\mathbf{C}\mathbf{T} + 2\mathbf{M}\dot{\mathbf{T}})\mathbf{B} \\ \mathbf{K}_B &= \mathbf{B}^{-1}\mathbf{T}^T(\mathbf{K}\mathbf{T} + \mathbf{C}\dot{\mathbf{T}} + \mathbf{M}\ddot{\mathbf{T}})\mathbf{B} \end{aligned} \quad (10)$$

are the Coleman transformed mass, damping/gyroscopic and stiffness matrices, respectively. If the system is isotropic, then \mathbf{A}_B is time-invariant, and a transient solution of equation (9) is

$$z_2 = e^{\mathbf{A}_B t} z_2(0) = \mathbf{V} e^{\mathbf{\Lambda} t} \mathbf{q}(0) \quad (11)$$

where $\mathbf{\Lambda}$ is a diagonal matrix containing the eigenvalues of \mathbf{A}_B , \mathbf{V} contains the corresponding eigenvectors as columns and $\mathbf{q}(0) = \mathbf{V}^{-1}z_2(0)$ are the initial conditions in modal coordinates. It is assumed that all eigenvectors are linearly independent.

The blade motion given in the inertial frame in equation (11) can be transformed back into the rotating frame using equation (6) as²¹

$$y_{T,ik} = e^{\sigma_k t} \left(A_{0,ik} \cos(\omega_k t + \varphi_{0,ik}) + A_{BW,ik} \cos((\omega_k + \Omega)t + \varphi_j + \varphi_{BW,ik}) + A_{FW,ik} \cos((\omega_k - \Omega)t - \varphi_j + \varphi_{FW,ik}) \right) \quad (12)$$

where $\varphi_j = 2\pi(j-1)/3$ and σ_k and ω_k are the modal damping and frequency of mode number k , respectively, given by the eigenvalue $\lambda_k = \sigma_k + i\omega_k$ with $i = \sqrt{-1}$. The amplitudes for degree of freedom number i were determined from the components of the eigenvector v_k given in multiblade coordinates of equation (8) as $A_{0,ik} = |a_{0,ik}|$ and

$$A_{BW,ik} = \frac{1}{2} \left((\text{Re}(a_{1,ik}) + \text{Im}(b_{1,ik}))^2 + (\text{Re}(b_{1,ik}) - \text{Im}(a_{1,ik}))^2 \right)^{1/2} \quad (13)$$

$$A_{FW,ik} = \frac{1}{2} \left((\text{Re}(a_{1,ik}) - \text{Im}(b_{1,ik}))^2 + (\text{Re}(b_{1,ik}) + \text{Im}(a_{1,ik}))^2 \right)^{1/2} \quad (14)$$

where the subscripts 0, BW and FW denote symmetric, backward whirling and forward whirling motion, respectively.

3.2. Classical Floquet analysis

Floquet analysis enables the solution of the periodic equations of motion directly without an explicit transformation. Equation (4) is written in first order form

$$\begin{aligned} \dot{y}_2 &= \mathbf{A} y_2 \\ \mathbf{A} &= \begin{bmatrix} \mathbf{0} & \mathbf{I} \\ -\mathbf{M}^{-1}\mathbf{K} & -\mathbf{M}^{-1}\mathbf{C} \end{bmatrix} \end{aligned} \quad (15)$$

where $y_2 = \{y^T \dot{y}^T\}^T$ is the state vector and \mathbf{A} is the T -periodic system matrix.

Floquet theory²² states that the solution to equation (15) is of the form

$$y_2 = \mathbf{U} e^{\mathbf{\Lambda} t} \mathbf{U}^{-1}(0) y_2(0) \quad (16)$$

where \mathbf{U} is a T -periodic matrix and $\mathbf{\Lambda}$ is a diagonal matrix. One way to construct this solution is to form a fundamental solution to equation (15) as

$$\boldsymbol{\varphi} = [\varphi_1 \quad \varphi_2 \quad \dots \quad \varphi_N] \quad (17)$$

over one period, $t \in [0; T]$, where N is the number of state variables, such that $\dot{\boldsymbol{\varphi}} = \mathbf{A}\boldsymbol{\varphi}$. The monodromy matrix defined as

$$\mathbf{C} = \boldsymbol{\varphi}^{-1}(0)\boldsymbol{\varphi}(T) \quad (18)$$

contains all modal properties, which can be extracted from the eigenvalue decomposition

$$\mathbf{C} = \mathbf{V}\mathbf{J}\mathbf{V}^{-1} \quad (19)$$

where \mathbf{V} contains the column eigenvectors \mathbf{v}_k of \mathbf{C} , which are all assumed to be linearly independent and \mathbf{J} is a diagonal matrix containing the eigenvalues ρ_k of \mathbf{C} , called the characteristic multipliers. The characteristic exponents $\lambda_k = \sigma_k + i\omega_k$ contain the frequency ω_k and damping σ_k and are related to the characteristic multipliers as $\rho_k = \exp(\lambda_k T)$. Because the complex logarithm is not unique, the frequency is not determined uniquely, and the principal frequency $\omega_{p,k}$ and the damping σ_k are defined from the characteristic multipliers as

$$\begin{aligned} \sigma_k &= \frac{1}{T} \ln(|\rho_k|) \\ \omega_{p,k} &= \frac{1}{T} \arg(\rho_k) \end{aligned} \quad (20)$$

where $\arg(\rho_k) \in]-\pi; \pi]$ is implied, resulting in $\omega_{p,k} \in]-\Omega/2; \Omega/2]$. Any integer multiple of the rotor speed can be added to the principal frequency to obtain a more physically meaningful frequency^{23,24}

$$\omega_k = \omega_{p,k} + j_k \Omega \quad (21)$$

a choice that also affects the periodic modal matrix \mathbf{U} in equation (16). This matrix \mathbf{U} contains the periodic mode shapes \mathbf{u}_k and is given as²⁴

$$\mathbf{u}_k = \boldsymbol{\varphi}\mathbf{v}_k e^{-\lambda_k t} \quad (22)$$

where the real part of λ_k is given by equation (20) and the imaginary part of λ_k is defined by equation (21) by selecting j_k such that \mathbf{u}_k is as constant as possible for degrees of freedom measured in the inertial frame.

Introducing the Fourier transform of the periodic mode shape

$$\mathbf{u}_k = \sum_{j=-\infty}^{\infty} \mathbf{u}_{jk} e^{ij\Omega t} \quad (23)$$

the transient solution in equation (16) can be written as a sum of harmonic components

$$\mathbf{y}_2 = \sum_{k=1}^N \sum_{j=-\infty}^{\infty} \mathbf{u}_{jk} e^{(\sigma_k + i(\omega_k + j\Omega))t} \mathbf{q}_k(0) \quad (24)$$

where $\mathbf{q}(0) = \mathbf{U}^{-1}(0)\mathbf{y}_2(0)$. Note that equation (12) is a special case of this expression for $j = -1, 0, 1$.

3.3. Implicit Floquet analysis

The implicit Floquet method is here described based on the detailed description in Bauchau and Nikishkov,¹² which focuses on computation of the characteristic multipliers from the state transition matrix $\boldsymbol{\Phi}(T, 0)$. It can be defined in classical Floquet theory as

$$\boldsymbol{\varphi}(T) = \boldsymbol{\Phi}(T, 0)\boldsymbol{\varphi}(0) \quad (25)$$

Using equation (18), the relationship between the state transition and monodromy matrices is derived as

$$\boldsymbol{\Phi}(T, 0) = \boldsymbol{\varphi}(0)\mathbf{C}\boldsymbol{\varphi}^{-1}(0) \quad (26)$$

showing that $\boldsymbol{\Phi}(T, 0)$ and \mathbf{C} have identical eigenvalues (characteristic multipliers), and their eigenvectors are related as $\mathbf{v}_k = \boldsymbol{\varphi}^{-1}(0)\mathbf{w}_k$, where \mathbf{w}_k represents the eigenvectors of $\boldsymbol{\Phi}(T, 0)$.

The key feature of the state transition matrix is that it defines the solution $\mathbf{y}_2(T) = \boldsymbol{\Phi}(T, 0)\mathbf{y}_2(0)$ for a time integration of the system equations (equation (15)) over one period T with initial conditions $\mathbf{y}_2(0)$. Hence, without knowing the state transition matrix, it is possible to obtain the product of it with an arbitrary vector (the initial state vector) by integration of

equation (15) over one period. The Arnoldi algorithm²⁵ is a method to approximate the eigenvalues and the eigenvectors of a matrix, say $\Phi(T, 0)$, using only the matrix multiplication with $\Phi(T, 0)$ to construct an m -sized subspace

$$\mathbf{P} = [\mathbf{p}_1 \quad \mathbf{p}_2 \quad \dots \quad \mathbf{p}_m] \quad (27)$$

that satisfies the orthonormality condition

$$\mathbf{P}^T \mathbf{P} = \mathbf{I} \quad (28)$$

and where the eigenvalues $\tilde{\rho}_k$ of the subspace projected state transition matrix

$$\mathbf{H} = \mathbf{P}^T \Phi(T, 0) \mathbf{P} \quad (29)$$

converge towards the eigenvalues ρ_k of $\Phi(T, 0)$ with the largest modulus as the size m of the subspace increases. The subspace eigenvectors $\tilde{\mathbf{w}}_k$ of \mathbf{H} projected back to the full state space converge towards the eigenvectors \mathbf{w}_k of $\Phi(T, 0)$, i.e. $\mathbf{w}_k \approx \mathbf{P} \tilde{\mathbf{w}}_k$. The Arnoldi algorithm proceeds as follows:

```

Choose an arbitrary vector  $\mathbf{p}_1$  with  $|\mathbf{p}_1| = 1$ 
for  $n = 1, 2, \dots, m$ 
   $\mathbf{a} := \Phi(T, 0) \mathbf{p}_n$ 
  (integration of equation (15) over  $t \in [0; T]$ )
   $\mathbf{b} := \mathbf{a}$ 
  for  $j = 1, 2, \dots, n$ 
     $h_{j,n} := \mathbf{p}_j^T \mathbf{a}$ 
     $\mathbf{b} := \mathbf{b} - h_{j,n} \mathbf{p}_j$ 
  end
  if  $n < m$ 
     $h_{n+1,n} := |\mathbf{b}|$ 
     $\mathbf{p}_{n+1} := \mathbf{b} / h_{n+1,n}$ 
  end
   $\mathbf{p}_{n+1} := \mathbf{p}_{n+1} - \sum_{j=1}^n (\mathbf{p}_j^T \mathbf{p}_{n+1}) \mathbf{p}_j$ 
end
    
```

The last step in the n -loop is an explicit re-orthogonalization to eliminate an otherwise progressing skewness of the subspace basis and thereby ensure convergence of the algorithm.¹² Note that \mathbf{H} with components $h_{j,n}$, $n = 1, \dots, m$, $j = 1, \dots, n$, is an upper Hessenberg matrix for which there exist efficient eigenvalue solvers. In practice, the Arnoldi algorithm is continued until a desired number of eigenvalues $\tilde{\lambda}_k$ with the largest modulus and their corresponding eigenvectors $\mathbf{P} \tilde{\mathbf{w}}_k$ of the state transition matrix $\Phi(T, 0)$ are converged to within a specific tolerance.

To construct the approximations to the periodic mode shapes (equation (22)), the $m \times m$ fundamental solution matrix $\tilde{\varphi}$ to the subspace projected system equations is written as

$$\tilde{\varphi} = \mathbf{P}^T [\varphi_1 \quad \varphi_2 \quad \dots \quad \varphi_m] \quad (30)$$

where φ_j is the solution of the full system (equation (15)) integrated over $t \in [0; T]$ for each initial condition \mathbf{p}_j , whereby $\tilde{\varphi}(0) = \mathbf{I}$ because of equation (28). The eigenvectors $\tilde{\mathbf{v}}_k$ of the subspace projected monodromy matrix $\tilde{\mathbf{C}} = \tilde{\varphi}^{-1}(0) \tilde{\varphi}(T)$ are therefore identical to the eigenvectors $\tilde{\mathbf{w}}_k$ of the subspace projected state transition matrix (equation (29)). The periodic mode shapes in the subspace are therefore similar to equation (22) given by

$$\tilde{\mathbf{u}}_k = \tilde{\varphi} \tilde{\mathbf{w}}_k e^{-\tilde{\lambda}_k t} \quad (31)$$

which by projection back into the full state space using $\mathbf{u}_k = \mathbf{P} \tilde{\mathbf{u}}_k$ yields the approximated periodic mode shapes of the full system

$$\mathbf{u}_k \approx [\varphi_1 \quad \varphi_2 \quad \dots \quad \varphi_m] \tilde{\mathbf{w}}_k e^{-\tilde{\lambda}_k t} \quad (32)$$

where $\tilde{\mathbf{w}}_k$ and $\tilde{\lambda}_k$ are the eigenvectors and characteristic exponents of \mathbf{H} , respectively.

3.4. Partial Floquet analysis

Partial Floquet analysis²³ is a system identification technique that operates on signals with the free response of the system, thus no knowledge of the system equations is necessary. The signals can be obtained by numerical simulation or from measurements.

Singular value decomposition is used to eliminate noise and extract the frequency and the damping of the most dominant modes from a matrix similar to the monodromy matrix assembled from a limited number of signals spanning several periods. The entries in this matrix can only be sampled once per period for periodic systems, which limits the accuracy because the signal damps away, decreasing the signal to noise ratio. Time-invariant systems can, however, be sampled once per time step. Therefore, partial Floquet analysis is combined with Coleman transformation of the signals,²⁶ such that the response resembles that of a time-invariant system. This approach increases the accuracy and the number of modes that can be extracted from a given signal. However, a careful choice of forcing that excites all modes of interest to a sufficient level is necessary to extract these modes accurately.

4. NUMERICAL RESULTS

The modal analysis methods described in the previous sections are applied to a BHawC model of a 2.3 MW wind turbine with three 45 m blades, hub height 80 m and nominal speed 16 rpm. The model has 381 structural degrees of freedom.

4.1. Isotropic system

The turbine is mounted with identical blades and runs in a vacuum neglecting gravity forces, so the system is isotropic. The deflection of the blades because of centrifugal forces is therefore constant in the blade frame. The constant steady state is found at a given azimuth position by solving equation (1) statically, including centrifugal forces from the constant rotor speed. In this way, a steady state with no transients is obtained, and the system matrices become exactly periodic.

4.1.1. Coleman transformation approach

Because the system is isotropic, a modal analysis can be performed on the Coleman transformed system matrix. The system matrices \mathbf{M} , \mathbf{C} and \mathbf{K} from equation (4) were extracted at a single azimuth angle and combined into the Coleman transformed system matrix of equation (9) from which the modal frequencies, damping and eigenvectors given in the inertial frame were extracted. The time-invariance of the system matrix was checked by calculation for several azimuth angles.

Figure 2(a) shows the lowest modal frequencies as a function of rotor speed where the frequency is normalized with the lowest modal frequency at 0 rpm. The modes were named according to their dominant motion determined from the eigenvector and the whirling amplitudes calculated from equations (13) and (14). The mode labels in Figure 2 first contain the

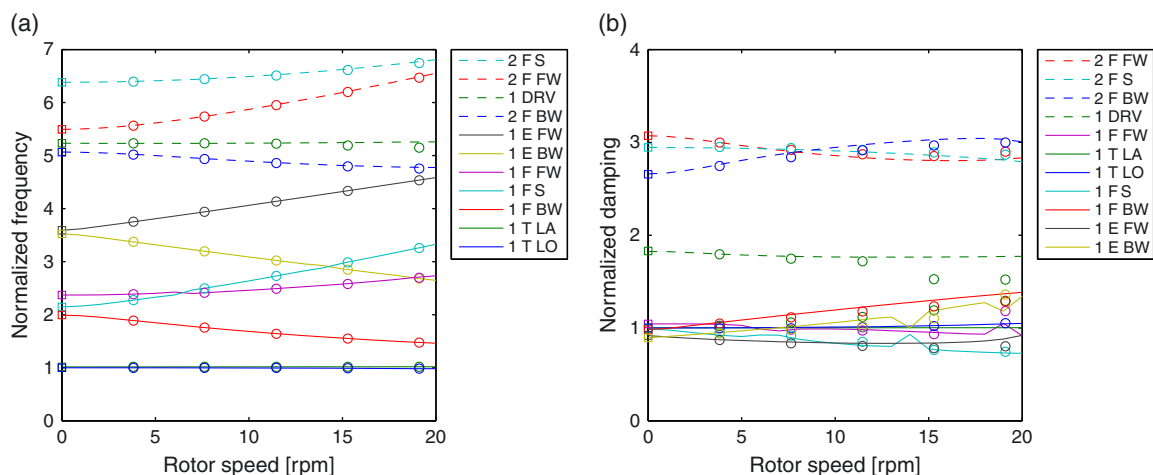


Figure 2. Frequency (a) and damping (b) as a function of rotor speed. Standstill eigenvalue analysis (squares), Coleman approach (lines), partial Floquet analysis (circles). Legend entries are ordered after the sequence at 0 rpm.

index of that particular mode, then ‘T’ for tower, ‘F’ for blade flapwise, ‘E’ for blade edgewise or ‘DRV’ for drivetrain and ‘LO’ for longitudinal, ‘LA’ for lateral, ‘BW’ for backward whirling, ‘FW’ for forward whirling or ‘S’ for symmetric. For comparison, the frequencies extracted from time simulations with the non-linear BHawC model using the partial Floquet method²⁶ are also shown. The agreement is within 0.4% except for modes coupling to the drivetrain, i.e. the drivetrain, edgewise and lateral tower modes, where the discrepancy is up to 2% at the highest rotor speed, which is caused by a difficulty with keeping the rotor speed exactly constant in the non-linear simulation because of the energy dissipated in the oscillation.

Figure 2(b) shows the damping as a function of rotor speed where the logarithmic decrement is normalized with the value for the first tower longitudinal mode at 0 rpm. The agreement in damping between the results from the linear model and the partial Floquet analysis applied to the non-linear model is within 6%, except for a discrepancy of up to 20% for modes coupling to the drivetrain. It must be noted that the purely structural damping of the modes is small, and thus, a small absolute difference leads to a high relative difference. The results also show that damping is more difficult to estimate than frequency using system identification.

4.1.2. Implicit Floquet analysis

For the implicit Floquet analysis, the system matrices in global coordinates in equation (4) were extracted from the steady state at 16 azimuth angles equally spaced over a rotor rotation. For interpolation to other azimuth angles, a least squares fit of a truncated Fourier series with eight terms was used. The fundamental solutions in equation (30) were integrated with a Newmark-type solver from initial conditions determined by the Arnoldi algorithm. The principal frequencies and damping were found from equation (20) where ρ_k are taken as the eigenvalues of the approximated state transition matrix. Figure 3 shows the real part σ_k of the characteristic exponents calculated at each Arnoldi step for a steady state at 12 rpm using a time step of $\Delta t = T/1024 = 0.0049$ s. The scattering of the highest damping values shows that the highest damped modes are spurious and do not represent actual eigenmodes of the system because of the approximate nature of the implicit Floquet analysis. To exclude these modes from the results, only modes satisfying a strict convergence criterion, where the absolute change of both damping σ_k and principal frequency $\omega_{p,k}$ is less than 10^{-10} between three successive steps, were retained. After 50 Arnoldi steps, 19 modes were converged. The modal frequencies were determined using equation (21) by adding $j_k \Omega$ to the principal frequency, where $j_k \Omega$ is the single non-vanishing harmonic component in a Fourier transform of the periodic mode shape for degrees of freedom on the tower calculated from equation (32) using the principal frequency $\omega_{p,k}$. The periodic mode shape components for degrees of freedom on the tower and the nacelle calculated with the modal frequency ω_k are thus constant. A detailed description of the process of frequency identification is given by Skjoldan and Hansen.²⁴

Figure 4 shows the difference in frequency calculated with the Coleman transformation approach and the implicit Floquet analysis with different integration time steps. The implicit Floquet results converge towards the Coleman transformation results for decreasing time steps, the error being roughly proportional to Δt^2 . Predominantly, the error increases with the modal frequency. A similar trend is seen for the damping.

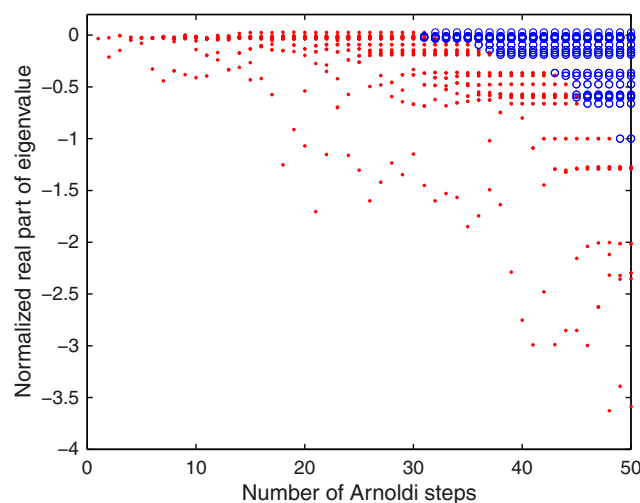


Figure 3. Magnitude of implicit Floquet characteristic multipliers as function of steps in Arnoldi algorithm. • non-converged eigenvalues, ○ converged eigenvalues.

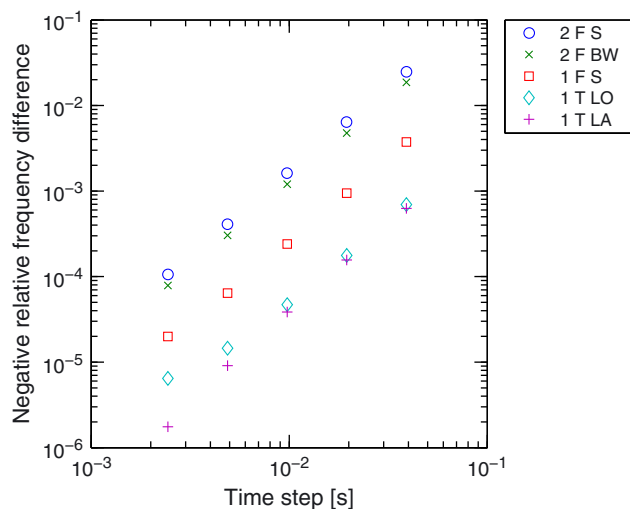


Figure 4. Relative difference in implicit Floquet frequency compared with Coleman approach frequency for selected modes as a function of implicit Floquet integration time step.

Figure 5 shows the dominant harmonic components \mathcal{U}_{jk} in equation (24) for the first flapwise forward whirling mode shape. The blade mode shape was transformed into substructure coordinates using equation (5) and contains the rigid body motion of the hub. The zoom factor in the lower right corner indicates how much each component has been enlarged. The ground fixed components in the mode shape are constant, consistent with the solution from the Coleman transformation approach. The mode shape for the blade has harmonic components at $j = -1, 0, 1$, corresponding to the forward, symmetric and backward whirling components, respectively, in the Coleman transformation approach. Thus, in a pure excitation of this mode at 12 rpm, according to equation (24), the tower vibrates with the normalized modal frequency $\omega' = 2.8$, and the blades dominantly vibrate with $\omega' - \Omega' = 2.2$ (FW) and to a lesser extent with $\omega' + \Omega' = 3.3$ (BW) and $\omega' = 2.8$ (S) (see Figure 2(a)).

4.2. Anisotropic system

To investigate the effects of an anisotropic rotor on the modal properties, a mass of 485 kg because of ice coverage defined by DIN-1055-5²⁷ is added along the length of blade 1. Figure 6 shows the resulting steady state when running the turbine at 16 rpm with a 10 m s^{-1} uniform wind field perpendicular to the rotor plane. Note that the wind is used only to drive the rotor, and the modal analysis is still purely structural. The steady state varies periodically both for the tower and the blades, and the blade motion for blade 1 is different from that of blades 2 and 3. The steady state was determined from a time simulation until transients have damped away, and system matrices were then extracted at each time step of the steady state simulation and interpolated onto integration time points using a truncated Fourier series with eight terms. The implicit Floquet analysis was carried out with an integration time step of $T/1024 = 0.0037 \text{ s}$ as described for the isotropic case. The frequencies were up to 4% lower than in the isotropic case because of the added mass on one blade. The change in damping was slightly more pronounced, up to a 17% decrease for the second flapwise forward whirling mode.

Figure 7 shows the harmonic components \mathcal{U}_{jk} with frequencies $j\Omega$ of the first flapwise forward whirling mode shape for the tower and blade 1. The tower mode shape now has several harmonic components compared with only one in the isotropic case. The component at $j = 0$ is similar in shape to the corresponding one for the isotropic case, but now the dominant component is at $j = -2$, and there is also a significant component at $j = -1$.

For the mode shape of blade 1, the harmonic components at $j = -1, 0, 1$ are similar to the corresponding ones in the isotropic case. However, now the amplitude of the dominant flapwise component at $j = -1$ for blade 1 is three times as high as for blades 2 and 3, and blades 2 and 3 move close to in-phase and in counter-phase with blade 1, as shown in Figure 8. Thus, in a pure excitation of this mode, the tower now vibrates dominantly with the normalized frequency $\omega' - 2\Omega' = 1.6$ in addition to the component at $\omega' = 2.8$. Blade 1 vibrates dominantly at $\omega' - \Omega' = 2.2$ as for the isotropic case and notably at $\omega' - 2\Omega' = 1.6$, $\omega' - 3\Omega' = 1.0$ and $\omega' + 3\Omega' = 4.5$ in addition to $\omega' + \Omega' = 3.3$ and $\omega' = 2.8$ as for the isotropic case.

The identification of the first flapwise forward whirling modal frequency was not done by making the tower mode shape as constant as possible, as in the isotropic case. Rather, the modal frequency was chosen to be close to the one for the

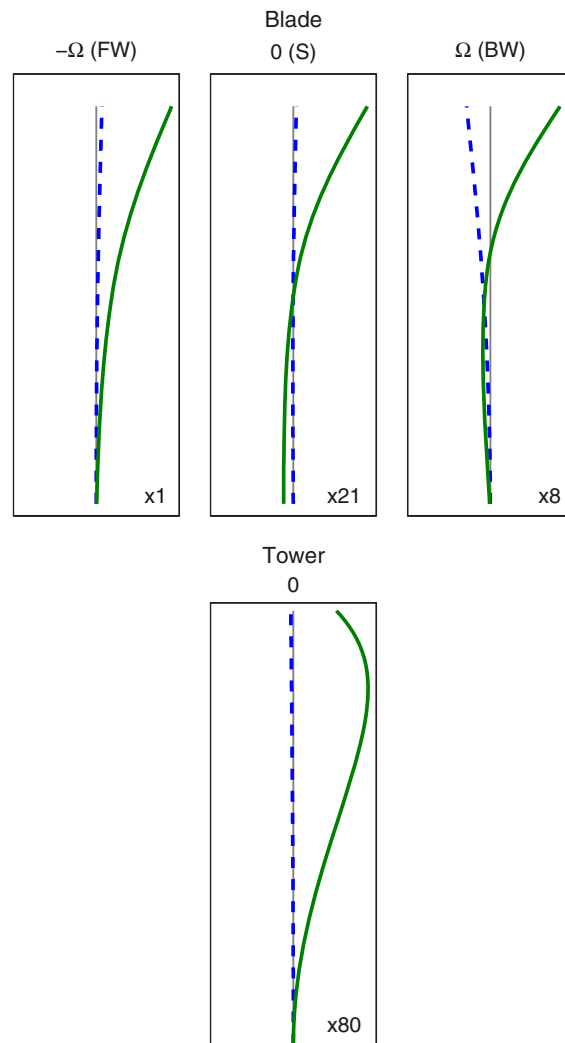


Figure 5. Amplitudes of harmonic components of the first flapwise forward whirling periodic mode shape for the isotropic rotor. Blades (top) — flapwise and - - edgewise, and tower (bottom) — longitudinal and - - lateral.

similar mode in the isotropic case. A more suitable criterion to give this result is to require that the mode shape with the rotor degrees of freedom in multiblade coordinates be as constant as possible.²⁸

The rotor with one ice-covered blade is an example of how an isotropic rotor can change the modal dynamics of the system. Other influences that could cause a similar behaviour is rotor stiffness unbalance, gravity loads, yaw error and wind shear. A two-bladed rotor is inherently anisotropic and requires a general approach like Floquet analysis.

5. DISCUSSION

This paper has presented several different methods for structural modal analysis of wind turbines. The Coleman approach is simple and fast, and its basis in a physical coordinate transformation means that the results are easily interpreted. Its speed makes it useful for doing parameter studies early in the design process. But it is only applicable to isotropic systems. Floquet analysis can be applied to examine special cases where anisotropic effects are suspected to change the modal parameters. The implicit Floquet analysis is an efficient implementation of Floquet analysis for systems with many degrees of freedom. In the example given, the most important modes are extracted after 50 integrations of the system over a rotor period, whereas 762 integrations would be needed for a classical Floquet analysis. Finally, the partial Floquet analysis, or another means of system identification, is useful to check the validity of the linearization.

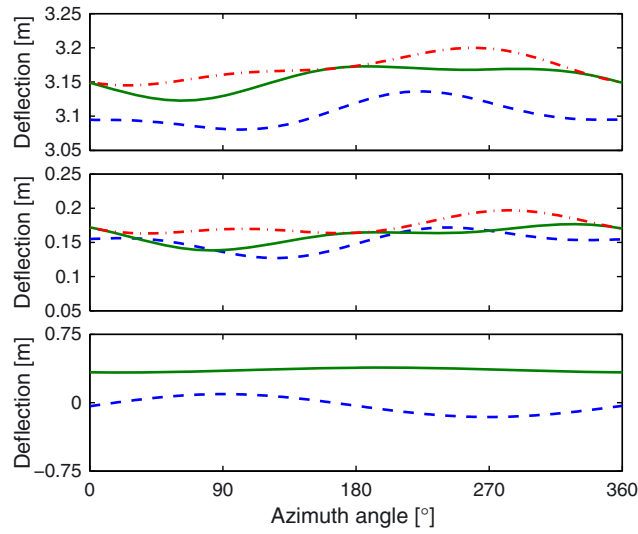


Figure 6. Steady state over one rotor period for the anisotropic rotor at 16 rpm. Blade tips flapwise (top) - - 1, — 2 and - - 3 and edgewise (middle) - - 1, — 2 and - - 3, and blade tips, tower top (bottom) — longitudinal and - - lateral.

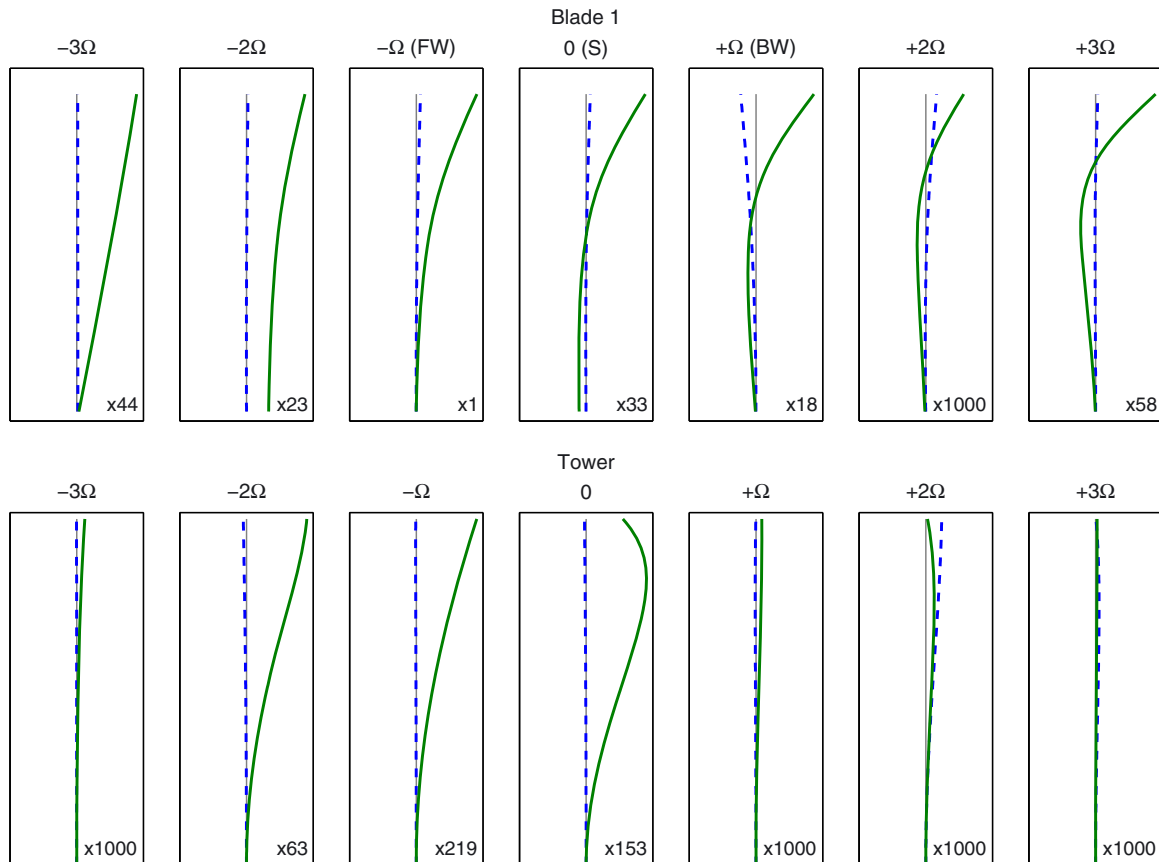


Figure 7. Amplitudes of harmonic components of the first flapwise forward whirling periodic mode shape for the anisotropic rotor with one blade covered with ice. Blade 1 (top) — flapwise and - - edgewise, and tower (bottom) — longitudinal and - - lateral.

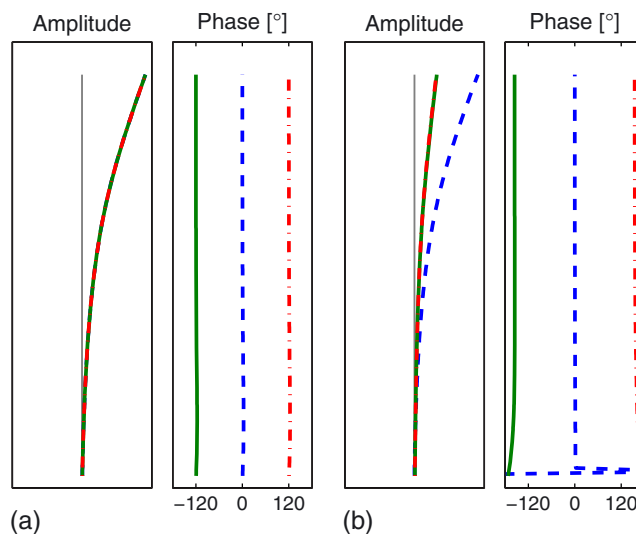


Figure 8. Amplitudes and phases of the harmonic component at $j = -1$ of the first flapwise forward whirling periodic mode shape for the isotropic rotor (a) and the anisotropic rotor (b). Blades - - 1, — 2 and - · - 3.

The work presented in this paper is part of an ongoing effort to obtain a full aeroelastic linear model of the non-linear code BHawC. The approach presented in this paper is readily extendable to a linear aeroelastic model. The linear model will aid in the understanding of the loads obtained from a non-linear response, of which many features can be explained from the linear modes.

6. CONCLUSION

Tangent matrices for structural modal analysis are extracted directly from the non-linear model of a wind turbine in a steady state. When the system is isotropic, the preferred approach is to use the Coleman transformation for describing the equations of motion in the inertial frame allowing direct eigenvalue analysis to extract the modal frequencies, damping and mode shapes. When the system is anisotropic, implicit Floquet analysis, reduces the computational burden associated with classical Floquet analysis, is applied to yield the lowest damped eigenmodes. The linearized model is validated from numerical results for a three-bladed turbine, showing a reasonable agreement for the frequencies and the damping between the Coleman approach and the partial Floquet analysis on the response of the non-linear model for modes not related to the drivetrain. The implicit Floquet results converge to the results from the Coleman approach with the deviation in frequency and damping roughly proportional to the square of the integration time step and increasing with the modal frequency. This finding shows the importance of precise time integration in implicit Floquet analysis. An analysis applied to an anisotropic system with one blade covered with ice shows a decrease in frequency up to 3% and changes in damping within 17%. It also reveals multiple harmonic components in the response of a single mode that will show up in measurements.

ACKNOWLEDGEMENT

This work has been partially supported by the Danish Ministry of Science, Technology and Innovation through the Industrial PhD programme.

REFERENCES

1. Larsen TJ, Hansen AM. How 2 HAWC2, the user's manual. *Technical Report Risø-R-1597(EN)*, Risø National Laboratory, Roskilde, Denmark, 2007.
2. Riziotis VA, Voutsinas SG. Fatigue loads on wind turbines of different control strategies operating in complex terrain. *Journal of Wind Engineering and Industrial Aerodynamics* 2000; **85**: 211–240.

3. Rubak R, Petersen JT. Monopile as part of aeroelastic wind turbine simulation code. *Proceedings of Copenhagen Offshore Wind*, Denmark, October 2005.
4. Riziotis VA, Voutsinas SG, Politis ES, Chaviaropoulos PK. Aeroelastic stability of wind turbines: the problem, the methods and the issues. *Wind Energy* 2004; **7**: 373–392. DOI: 10.1002/we.133
5. van Engelen TG, Braam H. TURBU offshore, computer program for frequency domain analysis of horizontal axis offshore wind turbines. *Technical Report ECN-C-04-079*, Energy Research Centre of the Netherlands, 2004.
6. Hansen MH. Aeroelastic stability analysis of wind turbines using an eigenvalue approach. *Wind Energy* 2004; **7**: 133–143. DOI: 10.1002/we.116
7. Bir G, Jonkman J. Aeroelastic instabilities of large offshore and onshore wind turbines. *Journal of Physics: Conference Series* 2007; **75**: 012069.
8. Kirchgässner B. ARLIS—a program system for aeroelastic analysis of rotating linear systems. *Proceedings of European Wind Energy Conference*, Hamburg, Germany, 1984; 253–258.
9. Matthies HG, Nath C. Dynamic stability of periodic solutions of large scale nonlinear systems. *Computer Methods in Applied Mechanics and Engineering* 1985; **48**: 191–202.
10. Stol K, Balas M, Bir G. Floquet modal analysis of a teetered-rotor wind turbine. *Journal of Solar Energy Engineering* 2002; **124**: 364–371.
11. Peters DA. Fast Floquet theory and trim for multi-bladed rotorcraft. *Journal of the American Helicopter Society* 1994; **39**: 82–89.
12. Bauchau OA, Nikishkov YG. An implicit Floquet analysis for rotorcraft stability evaluation. *Journal of the American Helicopter Society* 2001; **46**: 200–209.
13. Stol KA, Moll H-G, Bir G, Namik H. A comparison of multi-blade coordinate transformation and direct periodic techniques for wind turbine control design. *Proceedings of 47th AIAA Aerospace Sciences Meeting*, Orlando, FL, USA, 2009.
14. James GH, III, Carne TG, Lauffer GP. The natural excitation technique (NExT) for modal parameter extraction from operating wind turbines. *Technical Report UC-261*, Sandia National Laboratories, 1993.
15. Marrant B, van Holten Th. System identification for the analysis of aeroelastic stability of wind turbine blades. *Proceedings of European Wind Energy Conference*, London, UK, 2004.
16. Murtagh PJ, Basu B. Identification of equivalent modal damping for a wind turbine at standstill using Fourier and wavelet analysis. *Proceedings of the Institution of Mechanical Engineers, Part K Journal of Multi-body Dynamics* 2007; **221**: 577–589. DOI: 10.1243/14644193JMBD90
17. Skjoldan PF. Aeroelastic modal dynamics of wind turbines including anisotropic effects. PhD Thesis Risø-PhD-66(EN), Technical University of Denmark, 2011.
18. Nikravesh PE. *Computer-Aided Analysis of Mechanical Systems*. Prentice-Hall: New Jersey, 1988.
19. Johnson W. *Helicopter Theory*. Dover Publications: New York, 1980.
20. Hansen MH. Aeroelastic instability problems for wind turbines. *Wind Energy* 2007; **10**: 551–577. DOI: 10.1002/we.242
21. Hansen MH. Improved modal dynamics of wind turbines to avoid stall-induced vibrations. *Wind Energy* 2003; **6**: 179–195. DOI: 10.1002/we.79
22. Meirovitch L. *Methods of Analytical Dynamics*. McGraw-Hill: New York, 1970.
23. Bauchau OA, Wang J. Efficient and robust approaches to the stability analysis of large multibody systems. *Journal of Computational and Nonlinear Dynamics* 2008; **3**. DOI: 10.1115/12397690
24. Skjoldan PF, Hansen MH. On the similarity of the Coleman and Lyapunov-Floquet transformations for modal analysis of bladed rotor structures. *Journal of Sound and Vibration* 2009; **327**: 424–439. DOI: 10.1016/j.jsv.2009.07.007
25. Golub GH, van Loan CF. *Matrix Computations* (3rd edn). The Johns Hopkins University Press: Baltimore, MD, 1996.
26. Skjoldan PF, Bauchau OA. Determination of modal parameters in complex nonlinear systems. *Journal of Nonlinear and Computational Dynamics* 2010; in press.
27. DIBt. *Richtlinie für Windenergieanlagen*. Directive Reihe B, Heft 8, Deutsches Institut für Bautechnik, Berlin, Germany, 2004.
28. Skjoldan PF. Modal dynamics of wind turbines with anisotropic rotors. *Proceedings of 47th AIAA Aerospace Sciences Meeting*, Orlando FL, USA, 2009.